Capillary-Scale Monolithic Immunoaffinity Columns for Immunoextraction with In-Line Laser-Induced Fluorescence Detection

ARTICLE *in* ANALYTICAL CHEMISTRY · AUGUST 2005

Impact Factor: 5.64 · DOI: 10.1021/ac048142p · Source: PubMed

3 AUTHORS, INCLUDING:

Richard J Hodgson
University Health Network
19 PUBLICATIONS **433** CITATIONS

Anal. Chem. **2005,** *77,* 4404−4412

Capillary-Scale Monolithic Immunoaffinity Columns for Immunoextraction with In-Line Laser-Induced Fluorescence Detection

Richard J. Hodgson, Michael A. Brook, and John D. Brennan*

Department of Chemistry, McMaster University, Hamilton, Ontario, L8S 4M1, Canada

A bimodal meso/macroporous monolithic silica capillary column containing an entrapped antibody was prepared by a biocompatible sol−gel process and used for nanoflow immunoaffinity chromatography and immunoextraction studies. Stationary phases were prepared by combining the protein-compatible silane precursor diglycerylsilane with an aqueous solution containing 10 000 Da poly(ethylene glycol) and the antibody. An analytical method was developed that was capable of determining both the dissociation constant and binding site content for the anti-fluorescein antibody within the stationary phase. The assay showed that while the antibody residing in macropores was easily removed, ∼20% of initially loaded antibody remained active and accessible after several washes, consistent with the antibody being entrapped within the mesopores of the sol−gel matrix. The dissociation constants for fluorescein binding to the anti-fluorescein antibody were similar in solution and in the meso/macroporous silica, indicating that the entrapped antibody retained its native conformation within such a matrix. The mixture was loaded into a 250-μm-i.d. fused-silica capillary where the polymer phase separated from the silica followed by gelation of the silica. The capillary-scale immunoaffinity columns could be operated at low back pressure using a syringe pump and were capable of performing chromatographic separations that were dependent on the presence of the antibody within the stationary phase. Such columns could also be operated using in-line laser-induced fluorescence detection. The use of the capillary-scale monolithic columns for on-column immunoextraction and preconcentration is also demonstrated.

Protein-doped columns have been widely used for sample purification and cleanup,[1] chiral separations,[2] on-line proteolytic digestion of proteins,[3] development of supported biocatalysts,[4] and more recently for screening of compound libraries via the frontal affinity chromatography (FAC) method.[5,6] In all cases, the predominant method used to prepare protein-loaded columns has been based on covalent or affinity coupling of proteins to solid supports. However, the coupling of proteins to beads has several limitations, including the following: loss of activity upon coupling (unless measures are taken to control protein orientation and conformation); low surface area; potentially high back pressure (which may alter K_d values[7]); difficulty in the loading of beads into narrow-bore columns; problems with miniaturizing to very narrow columns (<50-μm i.d.); and difficulty in immobilizing delicate target proteins such as membrane-bound receptors.[6]

A relatively recent advance in chromatographic columns is the development of monolithic stationary phases based on either silica[8−12] or polymer[13] skeletons. These self-supporting columns do not require frits, have a bimodal pore structure that leads to high plate numbers, and have high through-pore volumes, which

* To whom correspondence should be addressed. Tel: (905) 525−9140 (ext. 27033). Fax: (905) 527-9950. E-mail: brennanj@mcmaster.ca. Internet: http://www.chemistry.mcmaster.ca/faculty/brennan.

(1) (a) Hage, D. S. *J. Chromatogr., B* **1998**, *715*, 3−38. (b) Hage, D. S. *Clin. Chem.* **1999**, *45*, 593−615. (c) Weller, M. G. *Fresenius J. Anal. Chem.* **2000**, *366*, 635−645. (d) Muronetz, V. I.; Sholukh, M.; Korpela, T. *J. Biochem. Biophys. Methods* **2001**, *49*, 29−47. (e) Baczek, T.; Kaliszan, R. *J. Biochem. Biophys. Methods* **2001**, *49*, 83−98. (f) Burgess, R. R.; Thompson, N. E. *Curr. Opin. Biotechnol.* **2002**, *13*, 304−308.

(2) (a) Hage, D. S.; Noctor, T. A. G.; Wainer, I. W. *J. Chromatogr., A* **1995**, *693*, 23−32 (b) Hofstetter, H.; Hofstetter, O. Schurig, V. *J. Microcolumn Sep.* **1998**, *10*, 287−291 (c) Hofstetter, O.; Lindstrom, H.; Hofstetter, H. *Anal. Chem.* **2002**, *74*, 2119−2125. (d) Fitos, I.; Visy, J.; Simonyi, M. *J. Biochem. Biophys. Methods* **2002**, *54*, 71−84.

(3) (a) Hsieh, Y. L.; Wang, H.; Elicone, C.; Mark, J.; Martin, S. A.; Regnier, F. *Anal. Chem.* **1996**, *68*, 455−462. (b) Wang, C.; Oleschuk, R.; Ouchen, F.; Li, J.; Thibault, P.; Harrison, D. J. *Rapid. Commun. Mass. Spectrom.* **2000**, *14*, 1377−1383. (c) Wang, S.; Regnier, F. E. *J. Chromatogr., A* **2001**, *913*, 429−436. (d) Peterson, D. S.; Rohr, T.; Svec, F.; Frechet, J. M. J. *J. Proteome Res.* **2002**, *1*, 563−568. (e) Peterson, D. S.; Rohr, T.; Svec, F.; Frechet, J. M. J. *Anal. Chem.* **2002**, *74*, 4081−4088. (f) Slysz, G. W.; Schriemer, D. C. *Rapid Commun. Mass Spectrom.* **2003**, *17*, 1044−1050.

(4) Prazeres, D.; Miguel F.; Cabral, J. M. S. In *Multiphase Bioreactor Design*; Cabral, J. M. S., Mota, M., Tramper, J., Eds.; Taylor & Francis Ltd.: London, U.K., 2001; pp 135−180.

(5) (a) Schriemer, D. C.; Bundle, D. R.; Li, L.; Hindsgaul, O. *Angew. Chem., Int. Ed. Engl.* **1998**, *37*, 3383. (b) Zhang, B.; Palcic, M. M.; Schriemer, D. C.; Alvarez-Manilla, G.; Pierce, M.; Hindsgaul, O. *Anal. Biochem.* **2001**, *299*, 173−182.

(6) (a) Baynham, M. T.; Patel, S.; Moaddel, R.; Wainer, I. W. *J. Chromatogr., B* **2002**, *772*, 155−161 (b) Moaddel, R.; Lu, L.; Baynham, M.; Wainer, I. W. *J. Chromatogr., B* **2002**, *768*, 41−53. (c) Moaddel, R.; Cloix, J.-F.; Ertem, G.; Wainer, I. W. *Pharm. Res.* **2002**, *19*, 104−107. (d) Moaddel, R.; Wainer, I. W. *J. Pharm. Biomed. Anal.* **2003**, *30*, 1715−1724.

(7) (a) Royer, C. A. *Prog. Biotechnol.* **2002**, *19*, 17−25. (b) Seemann, H.; Winter, R.; Royer, C. A. *J. Mol. Biol.* **2001**, *307*, 1091−1102.

(8) Schulte, M.; Lubda, D.; Delp, A.; Dingenen, J. *J. High Resolut. Chromatogr.* **2000**, *23*, 100−105.

(9) Cabrera, K.; Lubda, D.; Eggenweiler, H.-M.; Nakanishi, H. M. *J. High Resolut. Chromatogr.* **2000**, *23*, 93−99.

(10) Nakanishi, K.; Shikata, H.; Ishizuka, N.; Koheiya, N.; Soga, N. *J. High Resolut. Chromatogr.* **2000**, *23*, 106−110.

10.1021/ac048142p CCC: $30.25
Published on Web 06/10/2005

provide low back pressure and hence increased flow rates relative to bead columns. Together, these factors lead to shorter separation times and more efficient separations.[8−13] Monolithic columns have also been derivatized with covalently tethered proteins after fabrication and utilized for bioaffinity chromatography applications.[14]

More recent work on the development of protein-doped monolithic sol−gel columns has appeared from the groups headed by Zusman[15] and Toyo'oka.[16] Zusman's group has developed columns using glass fibers covered with antibody-doped sol−gel glass as a new support for affinity separation of tumor-associated antigens from blood. Toyo'oka's group has used capillary electrochromatography (CEC) both to prepare protein-doped sol−gel-based columns and to elute compounds. The columns were derived solely from TEOS or TMOS using very high water/silicon and protein/silicon ratios, resulting in a column with sufficiently large pores to allow flow of eluent when charge was applied. While this is a significant advance, all chromatography was done using electroosmotic flow via CEC, which separates compounds on the basis of a combination of charge, mass and affinity.

Recently, our group has demonstrated that a very mild and biocompatible sol−gel processing method can be used to entrap active proteins within a monolithic silica column containing a distribution of meso- and macropores.[17] In this method, a two-step processing method was used wherein a buffered solution containing the protein and poly(ethylene glycol) (as a porogen) was added to a hydrolyzed silica sol to initiate phase separation and silica gelation under conditions that were protein-compatible.[18] Capillary columns based on these materials were shown to be suitable for pressure-driven liquid chromatography and compatible with electrospray mass spectrometry (ESI-MS/MS) detection. However, such columns retained only a fraction of the initially loaded protein (~25%), presumably due to leaching of a fraction of protein that was loaded into the macropores. In addition, the columns could not be reused owing to exposure to low ionic strength conditions (necessary for ESI-MS analysis) and protein poisoning by high-affinity inhibitors.

In this work, we have prepared a series of mesoporous and meso/macroporous monolithic materials that contain the monoclonal anti-fluorescein antibody (AF) and have developed a fluorescence-based assay related to binding of fluorescein to AF to allow calculation of the dissociation constant and number of binding sites for AF entrapped in various types of sol−gel derived materials. The assay makes use of the large quenching of fluorescence intensity for fluorescein upon binding to AF and can be used to assess antibody properties even in nontransparent materials. Using this assay, we have assessed the role of both porosity and cationic additives on retention of AF within sol−gel derived materials. We show that columns containing entrapped AF can be used in conjunction with on-column laser-induced fluorescence (LIF) detection to allow for a much broader range of buffer conditions during affinity chromatography, compared with ESI-MS detection. The ability to modify the nature of the elution buffer without alteration of the LIF signal allows for more flexibility, with respect to modes of operation, than ESI-MS detection. Using monolithic anti-fluorescein columns we demonstrate frontal affinity chromatography and immunoextraction followed by compound release.

EXPERIMENTAL SECTION

Chemicals. Monoclonal mouse-anti-fluorescein IgG 4-4-20 and 8-hydroxypyrene-1,3,6-trisulfonic acid (pyranine) were purchased from Molecular Probes (Eugene, OR). Tetramethyl orthosilicate (TMOS, 99.9%) and 3-(aminopropyl)triethoxysilane (APTES) were obtained from Aldrich (Oakville, ON, Canada). Diglycerylsilane (DGS) was prepared from TMOS and glycerol as described previously.[19] Fluorescein, poly(allylamine) (PAM, MW 17 000), and poly(ethylene glycol) (PEG, MW 10 000) were obtained from Sigma (Oakville, ON, Canada). Fused-silica capillary tubing (250-μm inner diameter, 360-μm outer diameter, polyimide coated) was obtained from Polymicro Technologies (Phoenix, AZ). All water was distilled and deionized using a Milli-Q synthesis A10 water purification system. All other reagents were of analytical grade and were used as received.

Procedures. (1) Entrapment of AF in Silica Monoliths. A solution containing 16% (w/v) of 10 kDa PEG in 25 mM HEPES at pH 7.1 with 0.1 mg·mL^{-1} monoclonal mouse anti-fluorescein IgG 4-4-20 (absent in controls) was mixed with an equal volume of hydrolyzed DGS (prepared by mixing 1 g of DGS and 1 of mL water, followed by mixing and filtering through a 0.22-μm membrane), and 50 μL of the resulting solution was placed into the wells of a clear-bottom 96-well plate. In some cases, the buffer solution contained either 0.6 wt % APTES, 0.006 wt % PAM, or both. This resulted in final concentrations of 2.5 μg of anti-

(11) (a) Ishizuka, N.; Minakuchi, H.; Nakanishi, K.; Soga, N.; Tanaka, N. *J. Chromatogr., A* **1998**, *797*, 133−137. (b) Minakuchi, H.; Nakanishi, K.; Soga, N.; Ishizuka, N.; Tanaka, N. *J. Chromatogr., A* **1998**, *797*, 121−131. (c) Minakuchi, H.; Ishizuka, N.; Nakanishi, K.; Soga, N.; Tanaka, N. *J. Chromatogr., A* **1998**, *828*, 83−90. (d) Minakuchi, H.; Nakanishi, K.; Soga, N.; Ishizuka, N.; Tanaka, N. *Anal. Chem.* **1996**, *68*, 3498−3501. (e) Ishizuka, N.; Minakuchi, H.; Nakanishi, K.; Hirao, K.; Tanaka, N. *Colloids Surf.* **2001**, *187−188*, 273−279. (f) Tanaka, N.; Kobayashi, H.; Nakanishi, K.; Minakuchi, H.; Ishizuka, N. *Anal. Chem.* **2001**, *73*, 420A−428A.. (g) Tanaka, N.; Nagayama, H.; Kobayashi, H.; Ikegami, T.; Hosoya, K.; Ishizuka, N.; Minakuchi, H.; Nakanishi, K.; Cabrera, K.; Lubda, D. *J. High Resolut. Chromatogr.* **2000**, *23*, 111−116. (h) Motokawa, M.; Kobayashi, H.; Ishizuka, N.; Minakuchi, H.; Nakanishi, K.; Jinnai, H.; Hosoya, K.; Ikegami, T.; Tanaka, N. *J. Chromatogr., A* **2002**, *961*, 53−63.

(12) (a) Kato, M.; Sakai-Kato, K.; Toyo'oka, T.; Dulay, M. T.; Quirino, J. P.; Bennett, B. D.; Zare, R. N. *J. Chromatogr., A* **2002**, *961*, 45−51. (b) Dulay, M. T.; Quirino, J. P.; Bennett, B. D.; Zare, R. N. *J. Sep. Sci.* **2002**, *25*, 3−9. (c) Quirino, J. P.; Dulay, M. T.; Zare, R. N. *Anal. Chem.* **2001**, *73*, 5557−5563. (d) Dulay, M. T.; Quirino, J. P.; Bennett, B. D.; Kato, M.; Zare, R. N. *Anal. Chem.* **2001**, *73*, 3921−3926.

(13) (a) Xu, M.; Peterson, D. S.; Rohr, T.; Svec, F.; Frechet, J. M. J. *Anal. Chem.* **2003**, *75*, 1011−1021. (b) Hilder, E. F.; Svec, F.; Frechet, J. M. J. *Electrophoresis* **2002**, *23*, 3934−3953. (c) Xie, S.; Allington, R. W.; Frechet, J. M. J.; Svec, F. *Adv. Biochem. Eng./Biotechnol.* **2002**, *76*, 87−125.

(14) (a) Mallik, R.; Jiang, T.; Hage D. S. *Anal. Chem.* **2004**, *76*, 7013−7022.. (b) Jiang, T.; Mallik, R.; Hage D. S. *Anal. Chem.* **2005**, *77*, 2362−2372.

(15) Zusman R.; Zusman, I. *J. Biochem. Biophys. Methods* **2001**, *49*, 175−187.

(16) (a) Sakai-Kato, K.; Kato, M.; Toyo′oka, T. *Anal. Chem.* **2002**, *74*, 2943−2949. (b) Kato, M.; Sakai-Kato, K.; Matsumoto, N.; Toyo'oka, T. *Anal. Chem.* **2002**, *74*, 1915−1921. (c) Sakai-Kato, K.; Kato, M.; Toyo'oka, T. *Anal. Biochem.* **2002**, *308*, 278−284. (d) Sakai-Kato, K.; Kato, M.; Nakakuki, H.; Toyo'oka, T. *J. Pharm. Biomed. Anal.* **2003**, *31*, 299−309. (e) Sakai-Kato, K.; Kato, M.; Toyo'oka, T. *Anal. Chem.* **2003**, *75*, 388−393. (f) Kato, M.; Matsumoto, N.; Sakai-Kato, K.; Toyo'oka, T. *J. Pharm. Biomed. Anal.* **2003**, *30*, 1845−1850.

(17) Hodgson, R.; Chen, Y.; Zhang, Z.; Tleugabulova, D.; Long, H.; Zhao, X.; Organ, M. G.; Brook, M. A.; Brennan. J. D. *Anal. Chem.*, **2004**, *76*, 2780−2790.

(18) Jin, W.; Brennan, J. D. *Anal. Chim. Acta* **2002**, *461*, 1−36.

(19) (a) Brook, M. A.; Chen, Y.; Guo, K.; Zhang, Z.; Brennan, J. D. *J. Mater. Chem.* **2004**, *14*, 1469−1479. (b) Brook, M. A.; Chen, Y.; Guo, K.; Zhang, Z.; Jin, W.; Deisingh, A.; Cruz-Aguado, J.; Brennan, J. D. *J. Sol-Gel Sci. Technol.* **2004**, *31*, 343−348.

fluorescein per monolith, with 0.3 wt % APTES, 0.003 wt % PAM, or both present in some silica monoliths. Some sols were also prepared as described above with the omission of PEG to avoid macropore formation. All samples were stored for 3 days at 4 °C prior to testing.

(2) Fluorescence-Based Assay of Anti-Fluorescein Binding Sites. Assays were done for the anti-fluorescein antibody present in solution and when entrapped in mesoporous and macro/mesoporous silica materials. For solution assays, 12 identical anti-fluorescein antibody samples (100 μL each, 2.5 μg of antibody/well) were placed in a 96-well plate, and 100 μL each of fluorescein solutions (12 different concentrations in the range of 0−200 nM) were added to each of the 12 wells. The plates were shaken for 30 min to allow fluorescein to equilibrate with the anti-fluorescein. Fluorescence intensity was determined from each well using a Tecan Safire multiwell plate reader using top excitation at 488 nm (2.5-nm band-pass) and top-read emission at 513 nm (2.5-nm band-pass), with the signal averaged over 40 flashes.

For AF in silica, both the entrapped and leached fractions of the antibody were assayed. Microwell plates containing 12 identical entrapped antibody samples in 50-μL silica monoliths were first washed with a total of 6 × 100 μL of 25 mM Tris-HCl, pH 7.5 containing 50 mM NaCl (30 min/wash step). To test for the presence of leached antibody, all washes from identical monoliths were pooled and assayed for AF activity by adding 100 μL of wash solution to 100 μL of solutions containing various fluorescein concentrations, as described above for solution assays of AF. Background fluorescence was negligible as was the fluorescence of bound fluorescein; therefore, the *x*-intercept of the resulting plot of emission intensity versus initial fluorescein concentration (for saturating fluorescein concentrations) could be used to determine the concentration of AF contained in each pooled fraction. Assays of entrapped AF were done for washed materials by adding 150 μL of buffer containing various concentrations of fluorescein to the 50-μL monoliths, with a different fluorescein concentration present in each of 12 microwells (final fluorescein concentrations of 0−200 nM in 200 μL total volume). The samples were allowed to equilibrate for 3 h (longer equilibration times did not alter the results), and the total fluorescence intensity was determined using top-read fluorescence, as described above.

In all cases (free and entrapped AF), the total fluorescence intensity, F, was plotted against the total concentration of fluorescein added to the AF sample, [L], and the data was fit by nonlinear regression to the following equation (the derivation of this equation is provided in the Supporting Information):

$$F = m[\mathrm{L}] - m\left(\frac{(K_\mathrm{D} + [\mathrm{L}] + [\mathrm{P}]) - (K_\mathrm{D}^2 + [\mathrm{L}]^2 + [\mathrm{P}]^2 + 2K_\mathrm{D}[\mathrm{L}] + 2K_\mathrm{D}[\mathrm{P}] - 2[\mathrm{L}][\mathrm{P}])^{1/2}}{2}\right) \quad (1)$$

where [P] is the total concentration of antibody binding sites, K_D is the antibody dissociation constant, and m is the slope of asymptote, which corresponds to the fluorescence yield of free fluorescein.

(3) Column Fabrication. Fused-silica tubing (250-μm i.d., 360-μm o.d.) was treated with APTES to promote electrostatic binding of the silica monolith to the capillary, as previously described.[17] A solution containing 16% (w/v) of 10 kDa PEG in 100 mM HEPES at pH 7.0 with 0.25 mg·mL^{-1} monoclonal mouse anti-fluorescein IgG 4-4-20 (absent in control columns) was mixed with an equal volume of hydrolyzed DGS (prepared as described above), and the solution was pumped into ∼1 m of capillary. Note that it was important to use freshly prepared DGS and to ensure that the DGS was synthesized using anhydrous starting materials in order to obtain high-quality columns. Dialysis of the stock AF, to remove phosphate and adjust the pH, was necessary to obtain optimal gelation times and homogeneous columns. Following filling of capillaries, the sol underwent phase separation in ∼2.5 min, followed by gelation of the silica ∼1 min later. The resulting columns were aged with reservoirs of 50 mM HEPES buffer at each end, for 5 days, and then were cut into 10-cm segments (4.9-μL bed volume) immediately prior to use.

(4) Chromatography. Columns were first conditioned by passing a minimum of 10 bed volumes of chromatography buffer containing 50 mM Tris-HCl (pH 7.5) through the column to remove any residual glycerol, PEG, and loosely bound antibody. Columns were then tested in frontal mode by passing various concentrations of fluorescein in chromatography buffer through the columns and determining the breakthrough volume of the fluorescein using LIF detection (see below). For immunoextraction studies, bound fluorescein was rapidly eluted from the washed column using an elution buffer containing 50 mM Tris-HCl (pH 7.5) with 20% (v/v) methanol. The mobile phase was delivered using a Harvard PHD 2000 syringe pump operated at a flow rate of 5 μL·min^{-1}. Analyte infusion was accomplished using an Upchurch Nanopeak 10-port injection valve with two identical, 150-μL loops. The 2-loop, 10-port valve system allows a single syringe to deliver both buffer and buffer + analyte by switching between loops, yielding very reproducible transitions.

Detection of fluorescein was accomplished using a laser-induced fluorescence system. The bioaffinity column was connected directly to a 75-μm-i.d. fused-silica capillary, which was used as the detection cell. A tunable argon ion laser with a power output of 20 mW (Melles Griot) operated at 488 (fluorescein) or 454 nm (pyranine) was directed at a window that was burned into the 75-μm-i.d. fused-silica capillary to produce a detection volume of ∼20 nL. Emission was collected into a fused-silica optical fiber (400−μm core, 100-μm cladding, 0.40 numerical aperture, Fiberguide Industries SPC-400/500R), which was positioned against the capillary at a right angle to the laser radiation using a $X-Y-Z$ micrometer controlled translation stage (Newport). Fluorescence emission, originating at the distal end of the fiber, was captured by the fiber, and the fluorescence exiting the proximal end of the fiber was passed through a 500-nm long-pass filter and then focused onto the entrance slit of a monochromator (ScienceTech 9010, 200-mm focal length, F/3.5) using a second lens (60-mm focal length, 30-mm diameter, Melles Griot), which produced a 1.2-mm spot at the slit. Fluorescence at 515 nm was detected using a Hamamatsu R928 photomultiplier tube located in an analog housing (ScienceTech PMM-02) operated at 950 V. The fluorescence signal was collected as a function of time using a PC with software supplied by the manufacturer (SciSpec version 2.0 for

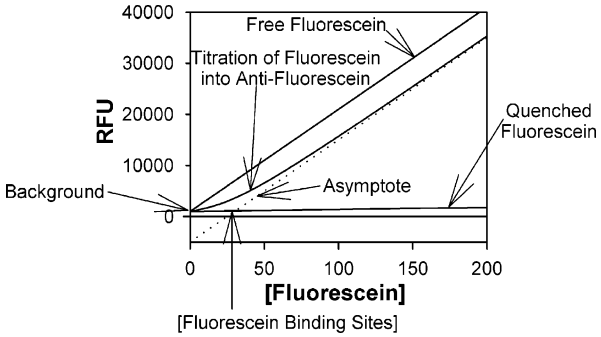

Figure 1. Schematic of a typical plot that would be obtained from quenching assays. The initial slope can be no smaller than the quenched fluorescein line. The asymptote is parallel to the line created by free fluorescein. The intersection of the asymptote and the quenched fluorescein line occurs at a concentration equivalent to the number of binding sites. Information about the K_D is contained in the shape of the curve and can be determined by least-squares regression using eq 1.

Windows). Both laser intensity and PMT voltage were decreased for detection of higher probe concentrations.

RESULTS AND DISCUSSION

Fluorescence Assay for Free AF. The binding of fluorescein to the anti-fluorescein antibody results in a >97% decrease in emission intensity, which provides a useful method to allow for detection of fluorescein binding.[20] In this study, a constant amount of antibody was titrated with varying amounts of fluorescein, leading to a response curve similar to that shown in Figure 1. In the absence of antibody, a linear increase in emission intensity with increasing fluorescein concentration is expected, as shown in the upper curve. In the case of saturating amounts of antibody, a much lower increase in intensity would be observed with increasing fluorescein concentration, as shown by the lower curve in Figure 1. In the case where there is a limited amount of antibody, the initial response upon addition of fluorescein will be similar to that obtained for the case of saturating antibody. However, as the antibody binding sites are saturated, the addition of further fluorescein will cause the change in emission intensity to become parallel to that obtained for free fluorescein in the absence of antibody. By fitting the slope of the response curve after saturating the antibody binding sites (dashed line in Figure 1), it is possible to determine the intersection of the asymptote and the quenched fluorescein responses curve, which indicates the number of fluorescein molecules bound and, hence, the number of antibody binding sites. Information about the K_D value of the antibody can also be obtained by nonlinear fitting of the entire response curve to eq 1.

Figure 2 demonstrates the use of *x*-intercepts as an indicator of the availability of fluorescein binding sites for an antibody in solution. Figure 2A shows the plots of fluorescence intensity against total fluorescein for increasing levels of antifluorescein antibody in solution (data for saturated antibody in the asymptotic region shown). As expected, the *x*-intercept shifts to higher fluorescein concentration values as the concentration of antibody is increased. Figure 2B shows the correlation between mass of

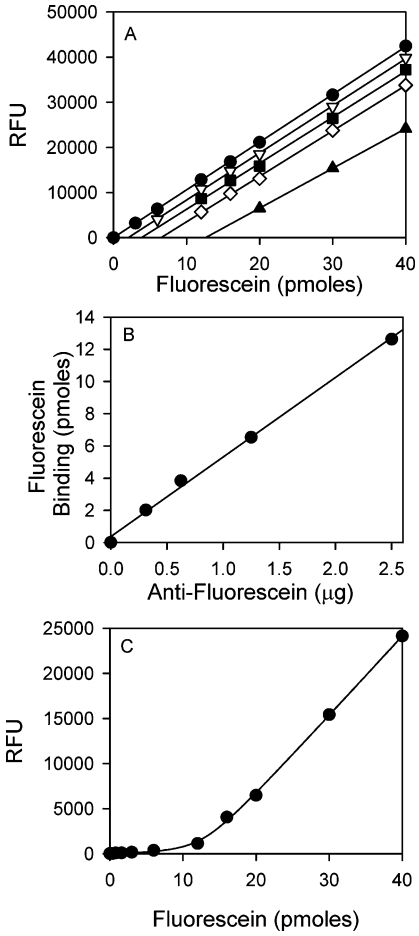

Figure 2. Use of *x*-intercept values as an indicator of the availability of fluorescein binding sites for an antibody in solution. (A) Fluorescence intensity against total fluorescein for increasing levels of antifluorescein antibody in solution. Data in asymptotic region shown. (●) No AF; (▽) 0.313. (■) 0.625, (◇) 1.25, and (▲) 2.5 μg of AF. (B) Correlation between the mass of antibody and measured antibody binding sites. (C) Validation of eq 1 for determining K_D values by using the fluorescein binding assay with a known amount of antibody in solution.

antibody and measured antibody binding sites. The curve shows the expected linear relationship (r^2 > 0.99), and the slope of 4.94 pmol of fluorescein/mg of anti-fluorescein is the specific activity of the antibody. This value is equivalent to 0.74 mol of fluorescein/mol of anti-fluorescein, based upon a M_r of 150 000 g/mol. Therefore, the antibody purchased from Molecular Probes is ~37% active considering that two binding sites are expected per antibody molecule. The specific activity determined here is consistent with the QC data, provided by Molecular Probes, for the antibody. These data show that the fluorescence assay can reliably determine the specific activity of the antibody.

To validate the applicability of eq 1 for determining K_D values, the fluorescein binding assay was run using a fixed amount of antibody in solution and generated the data shown in Figure 2C. The solid line shows the best fit to the data, and it is clear that the line passes through each of the points (r^2 > 0.99 for both runs). Fitting of the data provided identical concentrations of antibody for two independent assays (63.9 ± 1.7 and 64.8 ± 2.4 nM) and provided K_D values of 1.88 ± 0.40 and 1.89 ± 0.62 nM for the two assays, which are in excellent agreement with the

(20) Wang, R.; Narang, U.; Prasad, P.; Bright, F. V. *Anal. Chem.* **1993**, *65*, 5, 2671−2675.

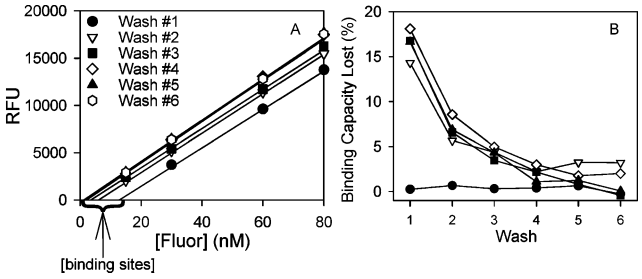

Figure 3. (A) Anti-fluorescein assay of six washes from one monolith type (DGS/PEG/APTES). Each wash consisted of 100 μL, or two monolith volumes, of buffer. Data were fit by linear regression. Where more antibody is present, the intercept is farther from the origin, and thus, each successive wash moves the intercept closer to the origin. Assays using low concentrations of fluorescein were not necessary because only the total amount of antibody was being measured, not the binding constant. (B) Calculated amount of antibody leached from each washing step using various monolith types. (●) DGS; (▽) DGS/PEG; (■) DGS/PEG/PAM; (◇) DGS/PEG/APTES; (▲) DGS/PEG/PAM/APTES.

Table 1. Amount of Active, Inactive, and Leached Antibody for Various Silica Compositions

	relative amounts (%)		
	active antibody entrapped[a]	active antibody in solution[b]	inactive or inaccessible antibody
DGS	79	2	19
DGS/PEG	20	33	47
DGS/PEG/PAM	28	29	43
DGS/PEG/APTES	16	39	45
DGS/PEG/PAM/APTES	23	31	46

[a] Based on [P] values shown in Table 2 for different monolithic materials. [b] Based on assay of wash solution.

dissociation constant for anti-fluorescein previously reported in the literature.[20] These results confirm that the fitting of eq 1 can provide reliable dissociation constants for AF.

Assays of Entrapped AF. Figure 3 shows an example of an anti-fluorescein assay applied to six consecutive washes obtained from a DGS/PEG/APTES monolith and shows that the assay can be used to assess the amount of antibody that leaches from the monolith in each wash cycle. As shown in Figure 3A, assays of initial washes provide data that are shifted relatively far from the origin, indicative of significant leaching, while assays of subsequent washes shift progressively toward the origin, indicative of less antibody being present in the wash solution. Figure 3B shows the calculated amount of antibody present in each wash solution for a series of different monoliths with varying composition. The data show that the highest degree of leaching is obtained in the first wash cycle (>15% of initially entrapped antibody) and is reduced to <5% of the initially loaded antibody by the sixth wash cycle. In summing the leached antibody for all washes, the total amount of antibody that leaches is generally in the range of 30−40% of the initial loading for all macroporous materials (see Table 1), demonstrating that the antibody is sufficiently small to leach from such pores even when only gentle washing is done. On the other hand, only ~2% of initially added antibody is able to leach from DGS-derived samples that contain only mesopores, showing that the antibody is unable to diffuse through such small pores.

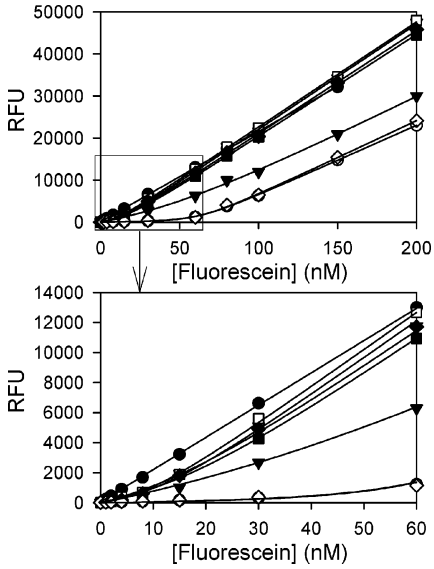

Figure 4. Quenching of fluorescein by entrapped anti-fluorescein. Lines are fit by least-squares regression to eq 1 so that binding constants can be derived. (●) Blank monolith (no AF); (○) solution test 1; (▼) DGS; (▽) DGS/PEG; (■) DGS/PEG/PAM. (□) DGS/PEG/APTES; (◇) DGS/PEG/PAM/APTES; (◇) solution test 2.

Previous studies have demonstrated that ~35% of the total pore volume of DGS/PEG-based materials resides in macropores with mean diameters in the range of 500 nm, while the remaining volume is present in mesopores with mean diameters of <10 nm.[17] Thus, the amount of antibody that leaches is consistent with the proportion of void volume present in macropores and provides strong evidence that leaching predominantly arises from protein that is present in macropores within the material. An important aspect of the entrapment of antibody in mesopores is that this situation will also provide a mass-dependent accessibility parameter for separation of small and large molecules in addition to the immunoselective binding, since large molecules cannot access the mesopores and will thus elute rapidly from the column.

The fact that the protein can leach is strong evidence for the lack of covalent bonds between the protein and the silica and is consistent with a wide body of literature that indicates the lack of such bonds.[18] However, antibodies can show significant restriction in dynamics when entrapped into mesoporous materials,[21] which has been suggested to implicate templating of silica around the antibody.[18] Thus, electrostatic or hydrogen-bonding interactions likely occur between the antibody and silica, even in the absence of PAM or APTES. The fact that the inclusion of charged additives, including APTES and PAM, does little to reduce the total amount of antibody that leaches would suggest that electrostatic binding between the protein and additive is not the predominant factor affecting leaching. However, it must be noted that the addition of PAM or APTES will not simply alter charge. Indeed, these materials will also accelerate gelation, which can lead to alterations in the extent of phase separation prior to gelation, and ultimately alter pore morphology in the resulting material.

Figure 4 shows assay data obtained directly from monoliths containing entrapped AF after the monoliths had been washed a

(21) Doody, M. A.; Baker, G. A.; Pandey, S.; Bright, F. V. *Chem. Mater.* **2000**, *12*, 1142−1147.

Table 2. Constants Derived from Curve Fitting Using Eq 1 for Plots of Fluorescence Intensity versus Fluorescein for AF Entrapped in Various Silica Compositions

	m	K_D (nM)	[P] (nM)
solution	168.3 ± 2.3	1.88 ± 0.4	63.9 ± 1.7
DGS	190.0 ± 11.5	31.2 ± 12.8	51.0 ± 14.3
DGS/PEG	251.3 ± 4.0	4.14 ± 3.25	12.8 ± 2.3
DGS/PEG/PAM	244.0 ± 2.2	7.75 ± 2.11	17.7 ± 1.4
DGS/PEG/APTES	250.5 ± 2.4	3.32 ± 2.1	10.0 ± 1.3
DGS/PEG/PAM/APTES	246.8 ± 3.9	8.87 ± 4.46	16.1 ± 2.6
fresh solution	177.4 ± 3.5	1.89 ± 0.62	64.8 ± 2.4

total of six times. It is clear that the response curves relating fluorescence intensity to total fluorescein concentration are generally shifted upward on the *y*-axis relative to the curves generated in solution, indicative of fewer binding sites or a lower binding affinity for fluorescein. It is possible that such changes may reflect slight alterations in the photophysics of fluorescein, which has been reported to undergo small alterations in its pK_a value upon entrapment.[22,23] However, this is not likely since the use of fluorescein has previously been shown to provide reliable binding constant data for entrapped AF.[20]

Table 2 shows the results of curve fitting to the data in Figure 4 and indicates several important findings. First, the total amount of active antibody binding sites that are accessible within the silica monoliths is always lower than the total number of antibody sites initially present in the monolith. In part this can be attributed to leaching of antibody; however, as shown in Table 1, the total amount of antibody binding sites summed over the entrapped and leached antibody is always less than 100% of the binding sites initially added to the silica and is typically in the range of 55% of total binding sites for the macroporous materials. Thus, on the order of 45% of initially added antibody is either inactive or inaccessible to analyte or both. While our data do not allow discrimination of inaccessible versus inactive antibody, it is possible to distinguish these situations using other methods, such as quenching of fluorescently labeled antibody.[24] These experiments are certainly useful in optimizing column materials but were not applied in this study. Second, the maximum amount of active entrapped antibody is obtained for mesoporous DGS materials (~80% of initially added antibody), while only 16−28% of initially added protein remains active within macroporous materials, regardless of the additive employed (note: PAM-doped materials appear to retain slightly more antibody, but monoliths prepared with this additive tended to be mechanically unstable). Third, the K_D value for entrapped AF was relatively close to the solution value for macroporous materials (generally 2−4-fold higher than in solution), while the K_D of AF in mesoporous materials was ~17-fold higher than the value obtained in solution. Such a finding is consistent with early work by Bright et al., who demonstrated a >10-fold increase in K_D values for AF entrapped in mesoporous materials derived from tetramethyl orthosilicate.[20] This may be related to mass transport limitations for delivery of the anionic fluorescein analyte through the anionic DGS-derived material.[25] On the basis of these findings, it was decided to further pursue the development of AF-doped columns using macroporous or DGS/PEG compositions.

Chromatography Using AF-Doped Monolithic Columns with LIF Detection. Meso/macroporous columns containing an initial loading of 3 pmol of AF in a 10-cm length were prepared using the DGS/PEG composition as described in the procedures and interfaced to the LIF system. After a 30-min wash, various concentrations of fluorescein were infused continuously at a flow rate of 5 μL/min, and breakthrough curves were monitored. Note that mesoporous columns prepared from pure DGS did not show any flow of eluent when a syringe pump was used for sample delivery. Thus, all experiments were done with macroporous columns.

Figure 5A shows breakthrough curves for columns containing from 1 to 200 nM fluorescein in an AF-loaded column (top panel) and shows the expected trend wherein the break-through time increases as the concentration of fluorescein decreases. It must be noted that these data were obtained by combining the breakthrough curves from a series of different AF columns, all cut from the same capillary. While methods exist to calculate K_D values from a single experiment on a single column,[26] we chose to use the single-experiment mode as a means of evaluating column to column reproducibility, which our data showed was better than 5% (RSD), allowing data from different columns to be combined. The data show that the LIF detection system has a detection limit of ~1 nM fluorescein (S/N = 3) prior to smoothing of data and significantly better after applying smoothing (~0.1 nM). The lower panels show several control experiments that indicate a lack of binding of fluorescein to blank columns and a lack of binding of pyranine (which has absorbance and emission properties similar to those of fluorescein but does not bind to AF) to either AF or blank columns. Together, these prove that the retention of fluorescein by the AF columns is due to the selective interaction of fluorescein with the entrapped AF antibody.

Figure 5B shows the determination of both the number of binding sites immobilized in the column and the dissociation of the bound antibody based on the change in breakthrough volume (given by the product of breakthrough time and flow rate) as a function of analyte concentration. Breakthrough volumes were determined as follows. The average of the postbreakthrough signal was used to normalize the raw data to 100%. The signal was then summed from $t = 0$ to n and compared to the sum of (100 − the data from $t = n$ to $t = 0$). The crossover point of these two sums represents a breakthrough point where the areas above and below the midpoint of the breakthrough are equal. The solid line is the best fit to the data points obtained using eq 2:

$$V = V_0 + \frac{B_t}{[\mathrm{A}] + K_d} \qquad (2)$$

where V_0 is the void volume (μL), V is the retention volume (μL),

(22) (a) Gulcev, M. D.; Goring, G. L. G. Rakic, M. Brennan, J. D. *Anal. Chim. Acta* **2002**, *457*, 47−59. (b) Tleugabulova, D.; Brennan, J. D. *J. Phys. Chem. B* **2004**, *108*, 10692−10699.

(23) Baker, G. A.; Watkins, A. N.; Pandey, S.; Bright, F. V. *Analyst* **1999**, *124*, 373−379.

(24) (a) Flora, K. K.; Brennan, J. D. *Chem. Mater.* **2001**, *13*, 4170−4179. (b) Sui, X.; Cruz-Aguado, J. A.; Chen, D. Y.; Zhang, Z.; Brook, M. A.; Brennan, J. D. *Chem. Mater.* **2005**, *17*, 1174−1182.

(25) Besanger, T. R.; Chen, Y.; Deisingh, A. K.; Hodgson, R.; Jin, W.; Stanislas, M.; Brook, M. A.; Brennan, J. D. *Anal. Chem.* **2003**, *75*, 2382−2391.

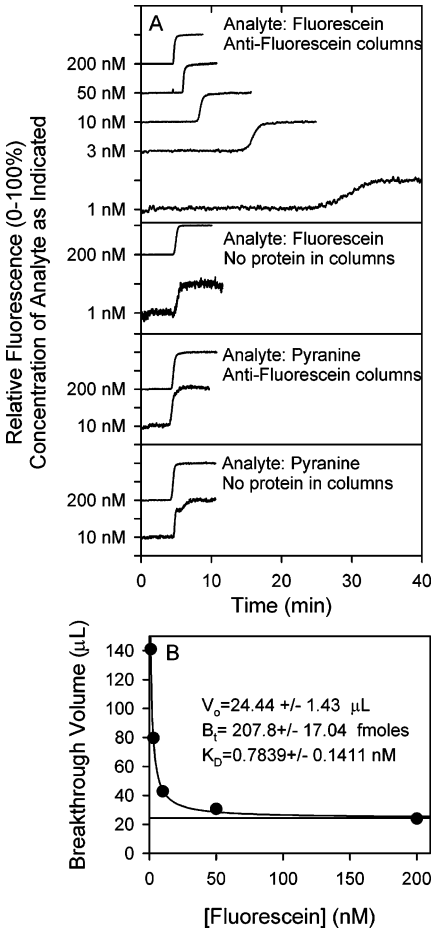

Figure 5. Determination of selectivity and antibody properties using FAC/LIF of fluorescein in AF and blank columns. Panel A shows frontal chromatograms obtained using increasing concentrations of fluorescein in an AF column (top panel) along with a series of selectivity controls, as noted in the figure. All frontal chromatograms were normalized and baseline offset to allow easier comparison of shifts in breakthrough time. Data for fluorescein binding to AF columns were run on individual columns, and the data were combined. Panel B shows the analysis of the changes in breakthrough volume for different ligand concentrations and the fit to the data using eq 2. Each column was 10 cm × 250 μm = 4.9 μL; flow rate 10 μL/min, All injections were done at 1 min. The LIF detector was detuned for the 50 and 200 nM measurements to keep the data on scale. Columns contained ~200 fmol of active AF, where applicable.

[A] is the analyte concentration (μM), K_d is the binding constant of the ligand to the protein (μM), and B_t is the total picomoles of binding sites immobilized in the column. Fitting the binding data to this equation leads to a calculated value of ~208 fmol of binding sites in the column. The columns were prepared with an initial antibody loading of 3 pmol; thus, only ~7% of the antibody remains active and accessible in the columns after column conditioning. This is much lower than the values of 16−28% obtained from the fluorescence-based assay and may reflect a higher loss of protein owing either to the much more efficient washing provided by one-way chromatographic flow, the pressure used to force eluent through the column, or both. However, this value is in the range reported by Hage et al. for covalent linkage of protein to polymer-based monolithic columns (1−6%).[14] The K_D value of 0.8 nM is ~2-fold lower than that obtained from the fluorescence-based assay of the antibody in solution and ~5-fold lower than was obtained for AF in different macroporous materials. The alteration in K_D values may reflect slight alterations in the pH or buffer composition when using chromatographic buffer relative to the plate-based assay, but is also potentially a sign of kinetic inaccessibility, which tends to lower K_d values as flow rate increases.[27] We are further investigating this effect and will report on our findings in a future paper. Interestingly, the data show that it is possible to obtain reasonable dissociation constants using columns with ~ 0.2 pmol of active protein present, which corresponds to a total loading of ~0.1 mg of active protein/g of silica from an initial loading of 1.2 mg·g^{-1} of antibody.

Figure 6 shows the use of the AF columns for bioselective immunoextraction of fluorescein from solution using AF-loaded columns (panel A), control data for blank columns (panel B), and the calibration curve relating emission intensity to fluorescein concentration (panel C). Columns were prepared from an initial solution of 3 pmol of antibody and contained a final concentration of ~200 fmol of active AF. Both AF and blank columns were examined using fluorescein or the nonbinding compound pyranine. Columns were first loaded at a flow rate of 150 μL·min^{-1} with 0.4 nM solutions of either fluorescein or pyranine in tap water (5 min, 750-μL loading), which is just below the detection limit for these probes when using the FAC mode of operation in the absence of data smoothing. The columns were then washed with 10 bed volumes of chromatography buffer at 5 μL·min^{-1} (10 min) to remove any unbound fluorophore. Data obtained from blank columns showed that 10 bed volumes of buffer was sufficient to remove any unbound species from the column (Figure 6B). A final stringent wash with elution buffer that contained 20% methanol (5 μL·min^{-1}) led to the generation of a large spike in fluorescence after 4 min for AF columns that were incubated with fluorescein, but not for AF columns incubated with pyranine or for blank columns loaded with fluorescein. Based on the height of the peak, the peak concentration during bump-off was ~8 nM (see panel C), which is ~20-fold higher than the calculated peak intensity values for 0.4 nM fluorescein, showing a preconcentration of the analyte. These data are consistent with selective immunoextraction of fluorescein using AF-loaded columns. Integration of the signal shows that a total of ~100 fmol of fluorescein was removed from the column during the bump-off step. Given that the columns had an initial loading of 210 fmol of binding sites and that we are operating at a fluorescein concentration that is close to the measured K_D value (0.8 nM), we should expect that roughly one-third of the available binding sites should be occupied (70 fmol). Given that there is a 30% error in the K_D value and a 20% error in the B_t value obtained from on-column experiments, the recovered value of 100 fmol is within error of the expected value of 70 fmol.

The use of 20% MeOH as the elution solvent is based on our intention to move toward MS-based detection with the immunoextraction columns to allow us to extend to nonfluorescent analytes, and thus, we used 20% methanol as the "bump" solution owing to its direct compatibility with MS. To ensure that this solvent did not lead to issues with reuse of columns, we ran five

(26) Schriemer, D. C. *Anal. Chem.* **2004**, *76*, 440A−448A.

(27) (a) Hage, D. S.; Thomas, D. H.; Beck, M. S. *Anal. Chem.* **1993**, *65*, 1622−30. (b) Nachman, M. *J. Chromatogr.* **1992**, *597*, 167−172. (c) Sportsman, J. R.; Liddil, J. D.; Wilson, G. S. *Anal. Chem.* **1983**, *55*, 771−775.

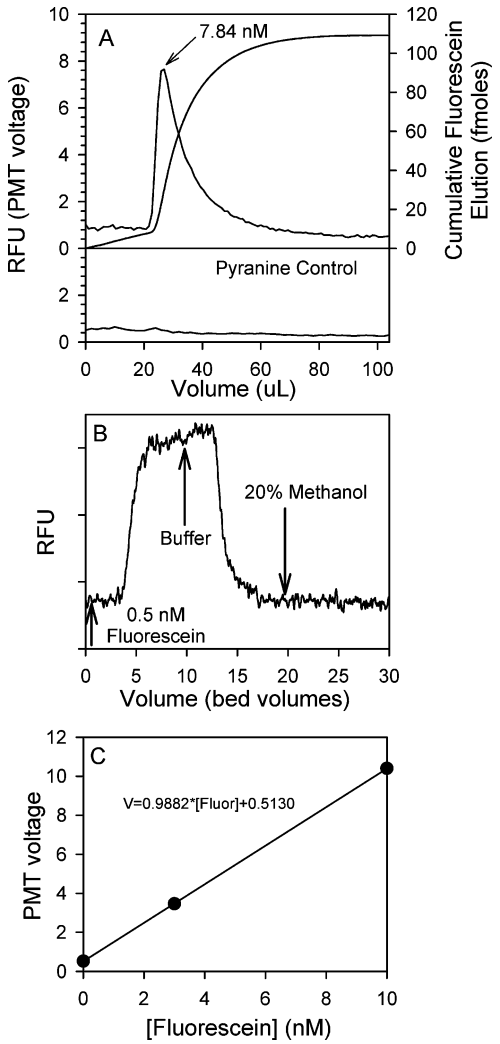

Figure 6. (A) Immunoextraction of fluorescein using an anti-fluorescein column. The columns were first loaded with 150 bed volumes of analyte and then washed with 10 bed volumes of chromatography buffer to remove unbound analyte. Bound analyte was then released from the column using 50 mM Tris-HCl, pH 7.5, containing 20% methanol starting at $t = 1$ min. Flow rate used was 150 μL·min^{-1} for analyte loading and 5 μL·min^{-1} for washing and elution. The smooth line shows the integration of the intensity data and indicates that 100 fmol of fluorescein was eluted during the bump-off step (see right-hand scale). (B) Decrease in fluorescence signal when infusion of 0.5 nM fluorescein is replaced with buffer, demonstrating the efficiency of the chromatographic washing step. (C) Calibration curve relating fluorescence intensity to concentration of fluorescein eluting from the column.

consecutive experiments involving extraction and bumping of a 1 nM fluorescein solution. As shown in Figure 7, the column could be reused several times, even after introduction of this solvent. Alternative bump solutions utilizing mild chaotropic agents could also be employed[28] but were not required in this work.

It should be noted that while the immunoextraction experiment required a total of ~20 min to perform, we could likely reduce this time by running all steps at higher flow rates. We have previously shown that such columns can be operated at flow rates of up to 500 μL·min^{-1},[17] and thus, it should be possible to run the entire immunoextraction experiment in a few minutes, if desired.

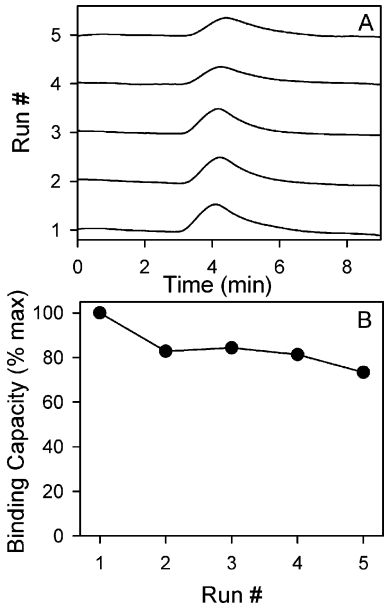

Figure 7. Reuse of columns after immunoextraction using 20% MeOH. (A) LIF signals obtained from five consecutive immunoextraction experiments using the same column. (B) Percentage of the initial signal recovered from each of the five consecutive immunoextraction experiments.

A key point to be noted in this work is the ability to directly detect the eluting analyte even in the presence of a high-ionic strength elution buffer. This highlights one of the important advantages of LIF detection over ESI-MS/MS detection,[17] since the latter detection method is not compatible with the use of high ionic strength buffers. Such columns should also be well suited for interfacing to matrix-assisted laser desorption/ionization (MALDI) MS/MS. We recently reported on the interfacing of capillary-scale monolithic bioaffinity columns to MALDI MS/MS for detection of inhibitors of an enzyme trapped in the column.[29] This work demonstrated it was possible to deposit eluent onto MALDI plates using a nebulizer-assisted electrospray method even when operating the columns at high ionic strength. Thus, it should be possible to interface the immunoextraction columns described herein to the same MALDI deposition system to allow preconcentration of analytes and sample cleanup prior to deposition on MALDI plates and thus obtain better detection limits. Our work in this area will be described in a future article.

CONCLUSIONS

The development and characterization of silica monolithic columns containing a bimodal distribution of meso- and macropores and entrapped antibody are demonstrated. Examination of antibody leaching using a new fluorescence-based assay shows that the antibody is retained in the mesopores within such columns but is essentially totally removed from the macropores within the columns. Inclusion of charged additives, which we expected would alter the electrostatic interactions of the antibody with the silica surface, had only a moderate effect on protein retention and altered monolith stability. Hence, the inclusion of cationic species may have a more complex effect on the sol−gel process than was

(28) Burgess, R. R.; Thompson, N. E. *Curr. Opin. Biotechnol.* **2002**, *13*, 304−308.

(29) Kovarik, P.; Hodgson, R. J.; Covey, T.; Brook, M. A.; Brennan, J. D. *Anal. Chem.* **2005**, *77*, 3340−3350.

originally intended. However, our data are consistent with the antibody being retained by physical entrapment in mesopores with diameters of <10 nm.

Chromatographic characterization of the columns demonstrated that macropores were essential to provide sufficient flow through the monoliths with low back pressure. Meso/macroporous monolithic silica columns containing entrapped anti-fluorescein antibody were shown to be able to selectively bind and retain fluorescein and could be used for selective immunoextraction of this small molecule. Formation of columns within 250-μm-i.d. fused-silica capillaries provided a system that required only very small amounts of protein ($\sim$ 0.2 pmol active protein) to produce a useful immunoaffinity column. Such columns are suitable for direct in-line laser-induced fluorescence detection of analytes and using such a detector can be operated at relatively high ionic strength. Columns were found to be reusable even after exposure to 20% MeOH, with a loss of binding activity of 20% over five cycles. Further work is underway to better understand the factors that affect column reusability, and the results of this work will be reported in due course.

The present work demonstrates the use of the monolithic columns for extraction of a small analyte (fluorescein), which was a useful model system to develop the LIF detection system and allow direct comparison of antibody behavior in columns and in monoliths. Thus, these columns should be useful for examination of protein−small molecule interactions, isolation of drug-like compounds and metabolites. Given the bimodal pore distribution within the silica monolith, it is not yet known if these columns can be used for the extraction of larger analytes (i.e., peptides or proteins), although previous studies with mesoporous materials have shown that polypeptides as large as 20 amino acids in length can access entrapped proteins.[30] Future studies will assess the molecular weight limitations in terms of analyte accessibility using a variety of fluorescently labeled peptides and proteins.

(30) Cruz-Aguado, J. A.; Chen, D. Y.; Brook, M. A.; Brennan, J. D. *Anal. Chem.* **2004**, *76*, 4182−4188.

ACKNOWLEDGMENT

The authors thank the Natural Sciences and Engineering Research Council of Canada, MDS-Sciex, the Canadian Foundation for Innovation, and the Ontario Innovation Trust and Research Corporation for financial support of this work. M.A.B. thanks the Canada Council for the Arts for providing a Killam Fellowship. J.D.B. holds the Canada Research Chair in Bioanalytical Chemistry.

SUPPORTING INFORMATION AVAILABLE

Additional information as noted in text. This material is available free of charge via the Internet at http://pubs.acs.org.

Received for review December 15, 2004. Accepted May 11, 2005.

AC048142P